Two-side surface photovoltage studies for implanted iron diffusion in silicon during rapid thermal anneal

I. Rapoport,[1,a)] P. Taylor,[2] J. Kearns,[3,b)] and D. K. Schroder[4]
[1]IR Process Solutions, Eugene, Oregon 97401, USA
[2]Wafer Reclaim Services, Vancouver, Washington 98682, USA
[3]NASA Headquarters, Washington, DC 20546, USA
[4]Department of Electrical Engineering, Arizona State University, Tempe, Arizona 85287, USA

(Received 30 August 2009; accepted 23 November 2009; published online 14 January 2010)

Two-side surface photovoltage (TS-SPV) based on measuring SPV from both wafer sides is proposed as the approach for silicon iron contamination monitoring. TS-SPV is applied to follow diffusion of implanted iron in a lightly doped p-type silicon during rapid thermal anneal (RTA). Good correlation is found between the iron distribution versus RTA conditions in the range of 375–1100 °C. The impact of thermal donors in silicon after RTA at below 700 °C is illustrated. The portion of iron detectable by SPV (FeB pairs) is found as a function of RTA time and temperature. Iron diffusion activation energy was evaluated for the interstitial ionized iron Fe_{i+} and for the interstitial neutral iron Fe_{i0}. Low thermal budget RTA combined with TS-SPV has been proven to be an effective iron contamination monitor to identify contamination sources, character, and location. © *2010 American Institute of Physics*. [doi:10.1063/1.3275045]

I. INTRODUCTION

Iron contamination is known as a yield limiting factor during silicon device manufacturing. Thermal oxide iron contamination leads to oxide degradation and decreases the oxide breakdown voltage. Once diffused into the silicon bulk, iron creates deep-level recombination centers, reducing the carrier lifetime and causing device malfunctions.[1,2]

Iron contamination during thermal processing originates from two major sources: iron diffusion from the wafer surface contaminated before thermal processes and iron cross contamination from the hardware components during thermal processing.[3] High-resolution surface photovoltage (SPV) iron mapping is frequently employed to track the metal contamination sources.[4,5]

Rapid thermal anneal (RTA) is widely used in modern silicon device manufacturing technology, making it important to study iron diffusion during RTA and to understand the impact of the thermal process conditions on interstitial iron ionization enabling FeB pair generation necessary for SPV.

As RTA thermal budgets are continually reduced for device processing, iron contaminants accumulate close to the wafer surface where the iron is initially introduced.

Measuring iron by SPV from both wafer sides is an effective means for monitoring iron contamination after thermal processing. Two-side SPV (TS-SPV) allows one to investigate the iron distribution throughout the wafer, and determine the contamination sources. When combined with low thermal budget anneals, TS-SPV serves as an effective fast-feedback metal contamination monitoring technique.

a)Electronic mail: igor.rapoport@cox.net.
b)This article is written in the co-author's personal capacity, and the views expressed do not represent the views of the United States Government.

II. EXPERIMENTAL SETUP

Measurements were made on boron-doped, 125 mm in diameter and 0.5 mm thick bare CZ silicon wafers with a resistivity of 20 Ω cm ($[B]=10^{15}$ atoms/cm^3) with low concentrations of interstitial oxygen atoms ($[O_i]<5\times10^{17}$ atoms/cm^3). Iron was implanted at a dose of $N_{Di}=5\times10^{10}$ atoms/cm^2 at an energy of $E=50$ keV. After implantation, the wafers were wet chemically cleaned including (a) Piranha etch at 120 °C, (b) HCl etch at 80 °C, and (c) standard SC-1 and SC-2 solutions, followed by intensive deionized water (DIW) rinse. The wafers were RTA annealed (see Fig. 1) in an oxygen ambient at temperatures from 375 to 1100 °C with temperature ramps of 50 °C/s. Thermal recipes were designed to diffuse iron from the implanted side, creating an iron concentration gradient across the silicon wafer.

The SPV preparation procedure included the oven anneal at 80 °C for 30 min to facilitate the FeB pair formation. The wafers were evaluated by measuring SPV on both wafer sides. The SPV preparation procedure was repeated before the second SPV measurement to ensure that all interstitial

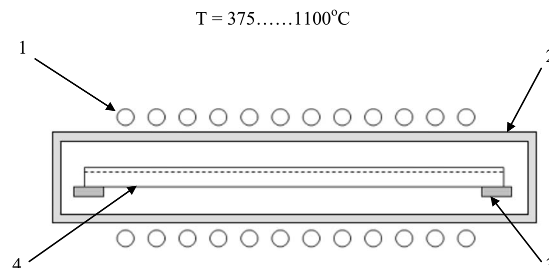

FIG. 1. Experimental schematic for iron implanted silicon wafers RTA: (1) infrared lamps, (2) quartz chamber, (3) quartz tray, and (4) iron ion implanted silicon wafer.

 © 2010 American Institute of Physics

Downloaded 14 Jan 2010 to 129.219.247.33. Redistribution subject to AIP license or copyright; see http://jap.aip.org/jap/copyright.jsp

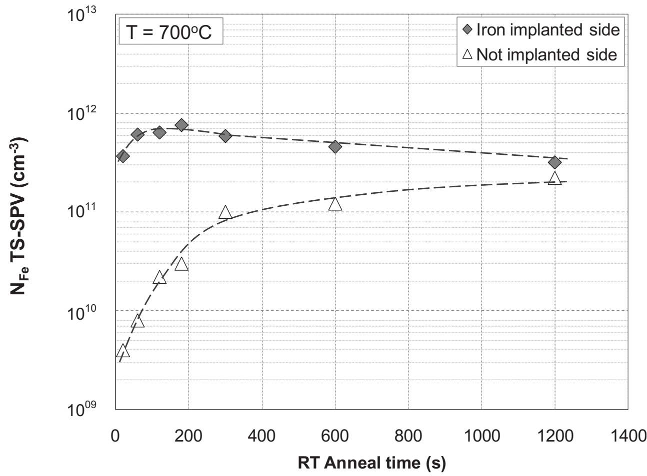

FIG. 2. Iron densities after RTA at 700 °C measured by TS-SPV on iron ion implanted (diamonds) and not implanted (triangles) silicon wafer sides. RTA treatment time varied from 20 s to 20 min.

ionized iron was paired with boron. Iron was quantified by measuring the SPV diffusion length before and after FeB pair dissociation using the equation

$$N_{\mathrm{Fe}} = 1.1 \times 10^{16}\left(\frac{1}{L_{\mathrm{after}}^2} - \frac{1}{L_{\mathrm{before}}^2}\right)\ \mathrm{cm}^{-3}, \qquad (1)$$

where L_{before} and L_{after} are the diffusion lengths in units of microns measured before and after FeB pair dissociation.[6]

The penetration depth z of the monochromatic light during SPV measurements is related to the photon flux density, photovoltage signal, and diffusion length by

$$\frac{\Phi_{\mathrm{eff}}}{V_{\mathrm{SPV}}} = \mathrm{const}\left(1 + \frac{z}{L}\right), \qquad (2)$$

where Φ_{eff} is the effective photon flux density entering the silicon, V_{SPV} is the photovoltage signal, and L is the diffusion length.[7]

The penetration depth of all relevant wavelengths is less than 200 μm (wafer thickness is approximately 500 μm). By measuring TS-SPV on both wafer sides, we obtain different iron concentration readings, reflecting the iron distribution throughout the silicon wafer.

III. RESULTS AND DISCUSSION

A. Iron diffusion profiles after RTA at 700 °C and correlation to TS-SPV results

Figure 2 shows the TS-SPV iron densities for iron-implanted wafers after RTA at 700 °C for annealing times from 20 s to 20 min. For annealing times shorter than 10 min, the SPV iron density measured on the iron-implanted wafer side is significantly higher than measured on the opposite wafer side. However, increasing the annealing time to 20 min at 700 °C evenly distributes the iron throughout the wafer.

Iron diffusion from the iron-implanted layer is given by the solution to Fick's second law

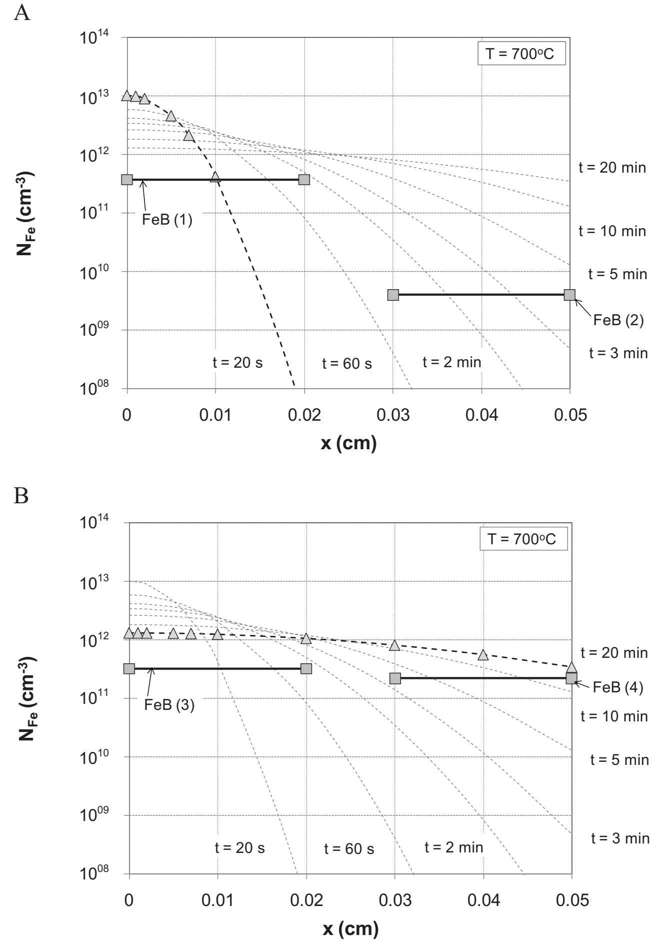

FIG. 3. Iron density diffusion profiles calculated (triangles) and TS-SPV FeB densities (squares) measured from the implanted [FeB(1) and FeB(3)] and from the not implanted side [FeB(2) and FeB(4)]: (a) after 700 °C RTA for 20 s and (b) after 700 °C RTA for 20 min.

$$C_{\mathrm{Fe}} = \frac{N_{\mathrm{Di}}}{(\pi D_{\mathrm{Fe}} t)^{1/2}} \exp\left(-\frac{x^2}{4D_{\mathrm{Fe}} t}\right), \qquad (3)$$

where N_{Di} is the iron implantation dose, D_{Fe} is the iron diffusion coefficient, t is the annealing time, and x is the distance from the iron-implanted surface.

The iron diffusion coefficient is given by

$$D_{\mathrm{Fe}} = 1.3 \times 10^{-3} \exp\left(-\frac{E_d}{kT}\right), \qquad (4)$$

where E_d is the iron diffusion activation energy (E_d =0.68 eV), k is Boltzmann's constant (k=8.625 $\times 10^{-5}$ eV/K), and T is the annealing temperature.[8]

Iron diffusion profiles after RTA at 700 °C were calculated using Eqs. (3) and (4) and are presented in Fig. 3 along with iron densities measured by TS-SPV (FeB). Good correlation is found between the calculated iron profiles and the SPV iron data after RTA at 700 °C. SPV measured iron density FeB(2)=4×10^9 cm^{-3} from the not implanted wafer side after RTA at 700 °C for 20 s illustrates the iron bulk contamination baseline in silicon before implantation.

Downloaded 14 Jan 2010 to 129.219.247.33. Redistribution subject to AIP license or copyright; see http://jap.aip.org/jap/copyright.jsp

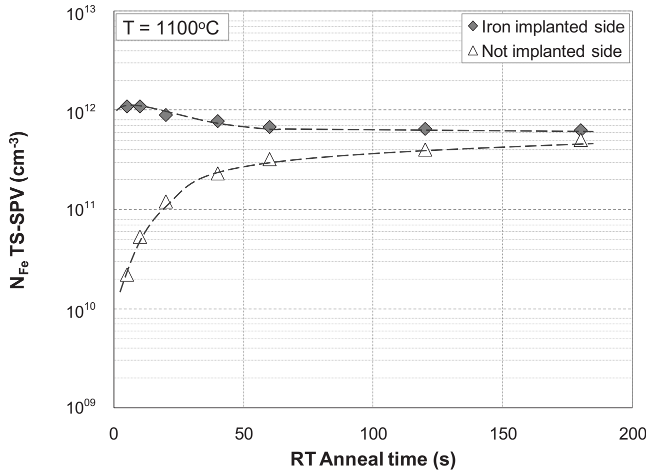

FIG. 4. Iron densities after RTA at 1100 °C measured by TS-SPV on the iron ion-implanted (diamonds) and not implanted (triangles) silicon wafer sides. RTA treatment time varied from 5 s to 3 min.

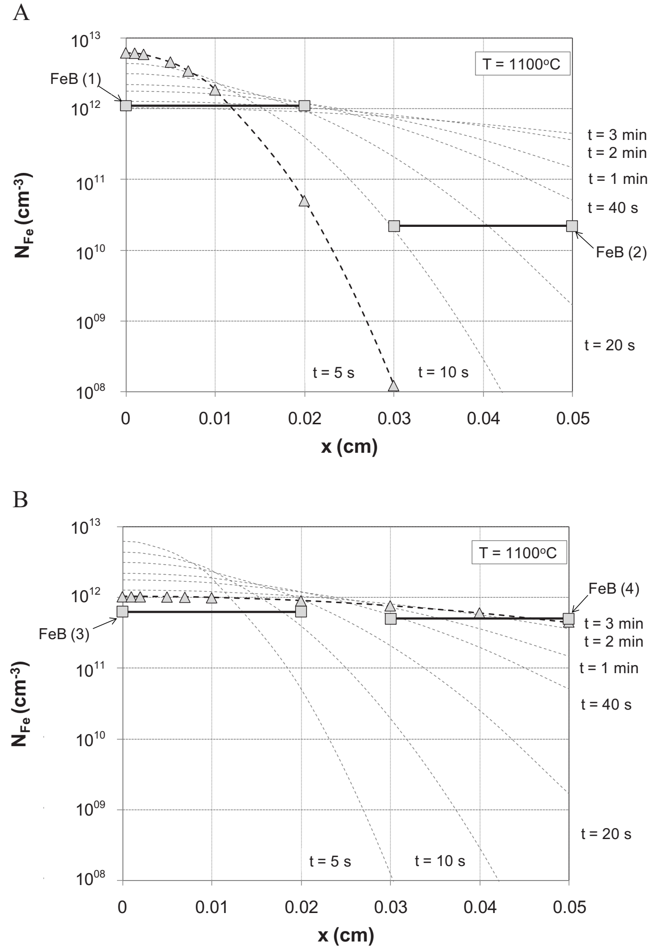

FIG. 5. Iron density diffusion profiles calculated (triangles) and TS-SPV FeB densities (squares) measured from the implanted [FeB(1) and FeB(3)] and from the not implanted side [FeB(2) and FeB(4)]: (a) after 1100 °C RTA for 5 s and (b) after 1100 °C RTA for 3 min.

B. Iron diffusion profiles after RTA at 1100 °C and correlation to TS-SPV results

Figure 4 shows the TS-SPV iron densities for iron-implanted silicon wafers after RTA at 1100 °C for annealing times from 5 s to 3 min. For annealing times over 1 min at 1100 °C, the implanted iron is almost evenly distributed across the wafer.

Iron diffusion profiles after RTA at 1100 °C were calculated using Eqs. (3) and (4) and are presented in Fig. 5 along with iron densities measured by TS-SPV (FeB). Good correlation is observed between the calculated iron profiles and the SPV iron data after RTA at 1100 °C. SPV measured iron density of 2×10^{10} cm^{-3} [level FeB (2) in fig. 5(a)] from the not implanted wafer side after RTA at 1100 °C for 5 s illustrates the driven-in iron surface contamination baseline on silicon wafer (before RTA).

C. Iron diffusion in silicon during RTA versus the annealing temperature studied by TS-SPV

Figure 6 presents the TS-SPV results after RTA at temperatures from 375 to 1100 °C. The annealing time is 5 min, except 3 min at 1100 °C, as determined by the RTA tool technical limits.

For the iron implanted wafer side after RTA below 700 °C, the iron detectable by SPV is limited by the iron activation in silicon (i.e., interstitial iron ionization to Fe^+ and diffusion toward B^- to create FeB pairs).

We should account for the impact of oxygen thermal donors (TDs) generated below 650 °C.[9] In the range from 700 to 775 °C the SPV measured iron distribution from the implanted side is governed primarily by diffusion (diffusion limited). Above 775 °C, the iron source from the implanted side starts depleting and the process becomes mainly dose limited.

For the not implanted side after annealing below 775 °C, the iron results can be explained as being diffusion limited and above 775 °C as being mainly iron dose limited. For the iron implanted silicon wafer side after RTA below 700 °C, any correlation between the SPV iron data (activation limited) and theoretical iron diffusion profiles is not expected because of the high TD density in silicon.

The iron diffusion equation (3) for the ion implanted wafer side ($x=0$) is given as

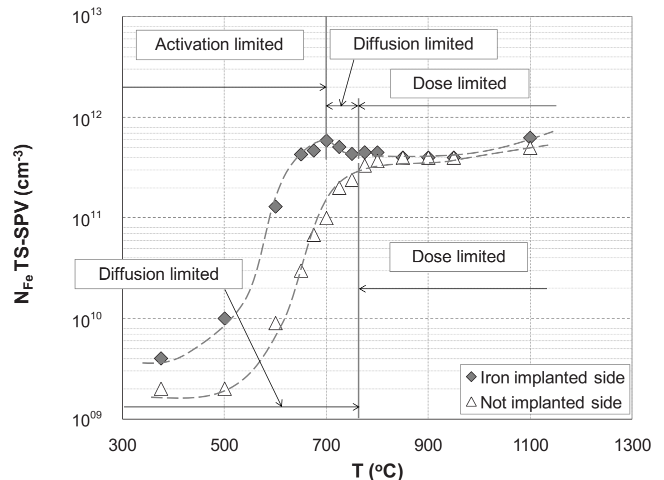

FIG. 6. Iron densities after RTA vs annealing temperature (in the range from 375 to 1100 °C) measured by TS-SPV on the iron ion implanted (diamonds) and not implanted (triangles) wafer sides. RTA treatment time is 5 min (except 3 min at 1100 °C, as limited by the RTA tool).

Downloaded 14 Jan 2010 to 129.219.247.33. Redistribution subject to AIP license or copyright; see http://jap.aip.org/jap/copyright.jsp

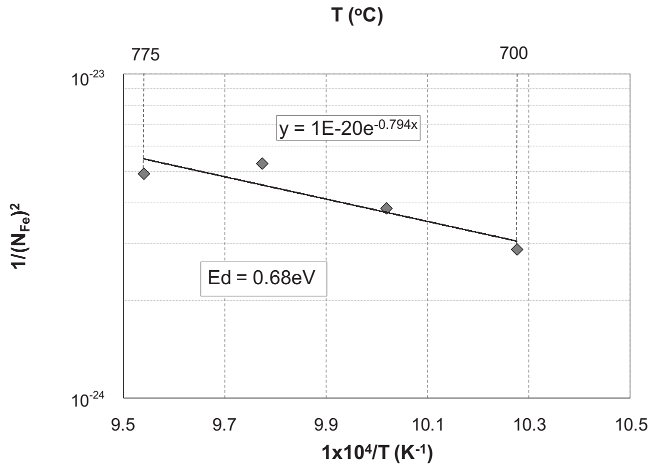

FIG. 7. The ratio $1/(N_{Fe})^2$ vs the reciprocal RTA temperature to determine the iron diffusion activation energy E_d. Here, N_{Fe} is the iron iron density measured by SPV from the ion implanted wafer side ($x=0$).

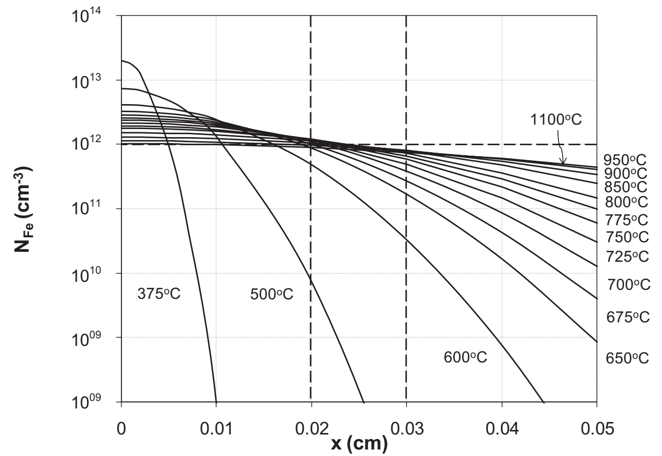

FIG. 8. Iron density diffusion profiles calculated after RTA. The annealing temperature is in the range from 375 to 1100 °C. The treatment time is 5 min (except 3 min for 1100 °C).

$$C_{Fe0} = \frac{N_{Di}}{(\pi D_{Fe} t)^{1/2}}, \tag{5}$$

where C_{Fe0} is the iron density on the wafer implanted side (can be represented by SPV measured data from the implanted side N_{Fe}), N_{Di} is the iron implantation dose, t is the annealing time (5 min), and D_{Fe} is the iron diffusion coefficient represented by Eq. (4).

From Eqs. (4) and (5), we suggest the following relationship:

$$D_{Fe} = 1.3 \times 10^{-3} \exp\left(-\frac{E_a}{kT}\right) \approx \frac{1}{(N_{Fe})^2}. \tag{6}$$

Figure 7 presents the ratio $1/(N_{Fe})^2$ versus the reciprocal RTA temperature. Here, N_{Fe} is the iron density measured by SPV from the ion implanted side ($x=0$). The iron diffusion activation energy is calculated as $E_d=0.68$ eV, which is in good correlation with E_d data from other sources.[8,10]

D. Yield of the SPV detectable iron versus the RTA temperature conditions: Interstitial neutral iron diffusion

Using Eqs. (3) and (4), we calculated the theoretical iron diffusion profiles from the iron ion implanted layer in silicon after RTA at different temperatures, shown in Fig. 8. Integrating the iron density diffusion profiles, we find the theoretical total iron density N_{Fe} (cm^{-2}) within the SPV penetration depth z [see Eq. (2)] from the ion implanted ($0<x<200$ μm) and not implanted silicon wafer sides (300 μm $<x<500$ μm).

The total iron density N_{FeB} (cm^{-2}) measured by SPV within the penetration depth z is calculated as

$$N_{FeB} = N_{FeB\text{-}SPV} \times z, \tag{7}$$

where $N_{FeB\text{-}SPV}$ (cm^{-3}) is the SPV measured iron density.

Figure 9 presents the theoretical total iron density N_{Fe} calculated from the iron diffusion profiles and the iron density N_{FeB} measured by SPV.

Knowing N_{Fe} (calculated from the iron diffusion profiles) and N_{FeB} (measured by TS-SPV) we could evaluate the yield of the SPV detectable iron in silicon versus the RTA temperature (see Fig. 10).

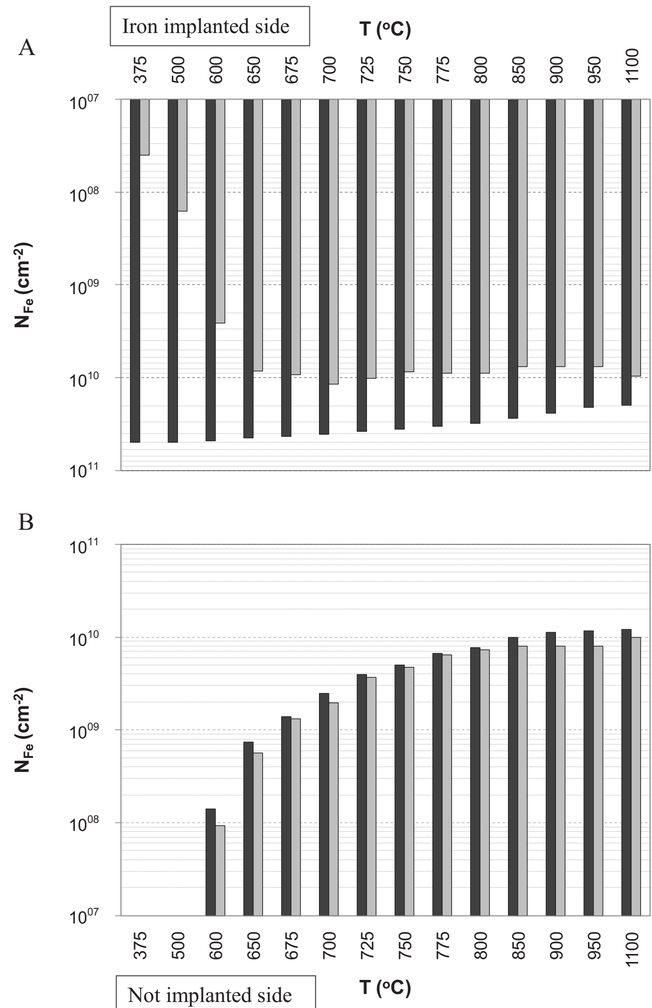

FIG. 9. Iron density N_{Fe} calculated from the theoretical iron diffusion profiles (dark bars) and iron density N_{FeB} measured by SPV (light gray bars) for (a) iron ion implanted and for (b) not implanted wafer sides.

Downloaded 14 Jan 2010 to 129.219.247.33. Redistribution subject to AIP license or copyright; see http://jap.aip.org/jap/copyright.jsp

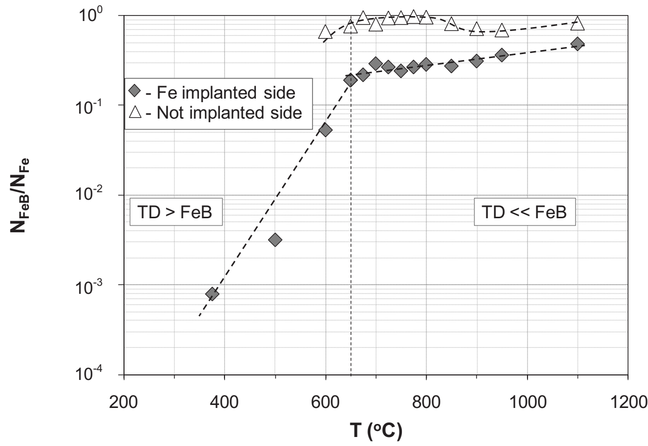

FIG. 10. The yield of the SPV detectable iron N_{FeB}/N_{Fe} measured from the ion implanted wafer side (diamonds) and from the not implanted wafer side (triangles) after RTA vs the anneal temperature, and the impact of TDs on the SPV results.

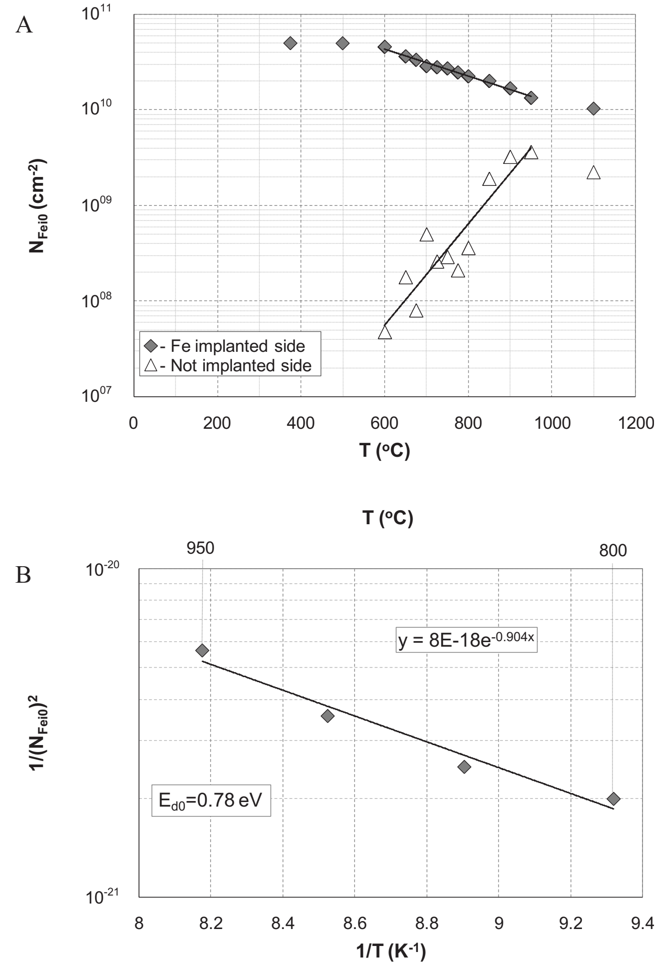

FIG. 11. Neutral interstitial iron diffusion calculation results: (a) N_{Fei0} after RTA vs the annealing temperature for the iron ion implanted and for not implanted silicon wafer sides and (b) the calculated ratio $1/(N_{Fei0})^2$ (at $x=0$, from the ion implanted wafer side) vs the reciprocal RTA temperature to evaluate the diffusion activation energy E_{d0}.

The total iron concentration in silicon is given by

$$N_{Fe} = N_{FeB} + N_{Fei} + N_{Fei0}, \quad (8)$$

where N_{FeB} is the density of interstitial iron associated with FeB pairs and detectable by SPV, N_{Fei+} is the density of interstitial iron ions, and N_{Fei0} is the density of interstitial iron neutrals.[11]

Low yield of the SPV detectable iron from the ion implanted wafer side after RTA at below 700 °C could be explained by the impact of TDs. During RTA above 700 °C TDs are annihilated.[12]

Assuming that 80 °C oven anneal before SPV is binding most of Fe_{i+} to FeB pairs, we interpret the rest of iron as neutral Fe_{i0}. The calculated N_{Fei0} versus the RTA temperature is presented in Fig. 11(a). Neutral interstitial iron densities from the iron ion implanted and from the not implanted wafer side are in good agreement with the diffusion theory. The shift in N_{Fei0} data after RTA at 1100 °C can be explained by the effective interstitial iron ionization during the anneal.

Using Eq. (6) we calculate the ratio $1/(N_{Fei0})^2$ (at $x=0$, from the ion implanted wafer side) versus the reciprocal RTA temperature in Fig. 11(b). The evaluated diffusion activation energy for Fe_{i0} in silicon is equal to $E_{d0}=0.78$ eV, and in good agreement with data from other sources.[8,10]

E. TS-SPV application to evaluate the iron contamination sources after RTA

TS-SPV technique was implemented for contamination sources monitoring after RTA at 700 °C. Boron-doped, 200 mm diameter bare CZ silicon wafers with a resistivity of 20 Ω cm ($[B]=10^{15}$ atoms/cm^3) with low interstitial oxygen ($[O_i]<5\times10^{17}$ atoms/cm^3) were handled using an iron contaminated vacuum wand touching both wafer sides. After that the silicon wafer was exposed to RTA at 700 °C for 2 min to drive-in the surface contamination [see the experiment schematic in Fig. 12(a)].

The SPV preparation procedure included thermal oxide strip in HF, followed by DIW rinse and oven anneal at 80 °C to facilitate the FeB pair generation. From the TS-SPV iron maps, we identified the location and side of the wafer on which the contamination was initially introduced [see SPV maps in Figs. 12(b) and 12(c)].

Implementing the low thermal budget anneal, followed by TS-SPV is a powerful technique to investigate the iron contamination sources after room temperature and low temperature operations as wafer cleaning, plasma etch, layer deposition, and other processes. Also it can be used to monitor contamination of the handling tools, susceptor, and materials that come in contact with silicon wafers.

IV. CONCLUSION

In studying the implanted iron diffusion dynamics by TS-SPV, we found good correlation between SPV iron results and theoretically calculated iron profiles when one takes into consideration that each SPV measurement is dominated by the local iron concentration within the SPV signal penetration depth.

Implementing TS-SPV studies, the diffusion activation energy was evaluated for iron interstitials ionized Fe_{i+} (E_d

Downloaded 14 Jan 2010 to 129.219.247.33. Redistribution subject to AIP license or copyright; see http://jap.aip.org/jap/copyright.jsp

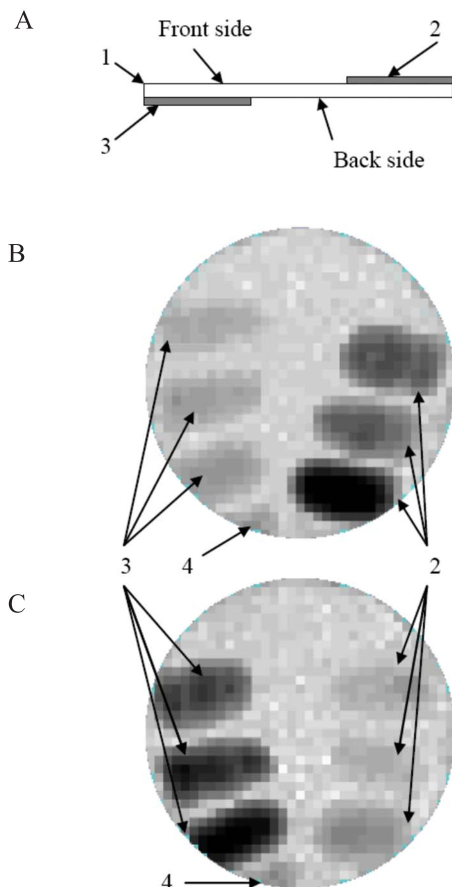

FIG. 12. (Color online) Wand marks study by TS-SPV after RTA at 700 °C for 2 min. The SPV iron maps color scale is from 10^9 cm^{-3} (white) to 10^{12} cm^{-3} (black). (a) Silicon wafer (1) view with wand marks from the front side (2) from the back side (3). (b) SPV iron map from the wafer front side. (c) SPV iron map from the wafer back side; (4) tweezers mark.

$=0.68$ eV) and for iron interstitial neutrals Fe_{i0} (E_{d0} $=0.78$ eV). Both are in good agreement with the E_d data from other sources.

The impact of thermal donors on the SPV detectable iron yield is illustrated after RTA below 650 °C. The SPV detectable iron yield in silicon versus RTA temperature was evaluated for iron ion implanted and not implanted wafer sides. An interstitial iron ionization increase was found after RTA at 1100 °C; this is helpful to increase the SPV detectable iron yield.

Knowledge about the iron diffusion dynamics during RTA is critical in designing the thermal recipes, and for iron drive-in and creating specific diffusion profiles before TS-SPV. TS-SPV is a powerful technique to monitor the iron contamination sources after the operations of wafer handling, wet recleaning, plasma treatment, layer deposition, and other processes. In particular, this technique is proven to be effective to study the contamination marks after RTA at 700 °C. TS-SPV is also a convenient tool for material studies to investigate the iron cross-contamination from other than silicon materials at elevated temperatures.

ACKNOWLEDGMENTS

The authors greatly appreciate the contribution from Benno Orschel to prepare this publication. Developed by Benno Orschel, the ZEBRA method was an important SPV technique improvement, enabling to implement the high accuracy and low detection limit iron measurements for TS-SPV approach.

The authors appreciate Chuck Hudak of the Core Systems for the assistance with the iron ion implantation to prepare the iron contaminated silicon samples of high quality.

[1] A. A. Isratov, H. Hieslmair, and E. R. Weber, Appl. Phys. A: Mater. Sci. Process. **70**, 489 (2000).
[2] A. A. Isratov, H. Hieslmair, and E. R. Weber, Appl. Phys. A: Mater. Sci. Process. **69**, 13 (1999).
[3] I. Rapoport, P. Taylor, B. Orschel, and J. Kearns, AIP Conf. Proc. **772**, 103 (2005).
[4] G. Zoth and W. Bergholz, J. Appl. Phys. **67**, 1 (1990).
[5] A. Cacciato, S. Vleeshouwers, and S. Evseev, J. Electrochem. Soc. **145**, 701 (1998).
[6] D. K. Schroder, *Semiconductor Material and Device Characterization* (Wiley, New York, 1998).
[7] J. Lagowski, A. M. Kontkiewicz, and L. Jastrzebski, Appl. Phys. Lett. **63**, 2902 (1993).
[8] K. Graff, *Metal Impurities in Silicon-Device Fabrication* (Spinger-Verlag, Berlin, 1995), p. 67.
[9] D. K. Schroder, C. S. Chen, J. S. Kang, and X. D. Song, J. Appl. Phys. **63**, 1 (1988).
[10] T. Heiser and A. Mesli, Appl. Phys. Lett. **58**, 2240 (1991).
[11] W. Wijaranakula, J. Electrochem. Soc. **140**, 275 (1993).
[12] H. J. Stein, S. K. Hahn, and S. C. Shatas, J. Appl. Phys. **59**, 10 (1986).

Downloaded 14 Jan 2010 to 129.219.247.33. Redistribution subject to AIP license or copyright; see http://jap.aip.org/jap/copyright.jsp